CANCER

Oncogenic JAK2^{V617F} causes PD-L1 expression, mediating immune escape in myeloproliferative neoplasms

Alessandro Prestipino,[1,2]* Alica J. Emhardt,[1]* Konrad Aumann,[3] David O'Sullivan,[4] Sivahari P. Gorantla,[1] Sandra Duquesne,[1] Wolfgang Melchinger,[1] Lukas Braun,[1] Slavica Vuckovic,[5,6] Melanie Boerries,[7,8,9] Hauke Busch,[7,10] Sebastian Halbach,[7] Sandra Pennisi,[1,2] Teresa Poggio,[1,2] Petya Apostolova,[1,11] Pia Veratti,[1,8,9] Michael Hettich,[12] Gabriele Niedermann,[12] Mark Bartholomä,[13] Khalid Shoumariyeh,[1] Jonas S. Jutzi,[1,14] Julius Wehrle,[1,8,9,11] Christine Dierks,[1] Heiko Becker,[1] Annette Schmitt-Graeff,[3] Marie Follo,[1] Dietmar Pfeifer,[1] Jan Rohr,[15] Sebastian Fuchs,[15] Stephan Ehl,[15] Frederike A. Hartl,[2,16] Susana Minguet,[2,15,16] Cornelius Miething,[1,8,9] Florian H. Heidel,[17,18] Nicolaus Kröger,[19] Ioanna Triviai,[19] Tilman Brummer,[7,8,9,16] Jürgen Finke,[1] Anna L. Illert,[1] Eliana Ruggiero,[20] Chiara Bonini,[20] Justus Duyster,[1,8,9] Heike L. Pahl,[1] Steven W. Lane,[5,21,22] Geoffrey R. Hill,[5,21,22] Bruce R. Blazar,[23] Nikolas von Bubnoff,[1,8,9] Erika L. Pearce,[4] Robert Zeiser[1,8,9,16†]

Recent evidence has revealed that oncogenic mutations may confer immune escape. A better understanding of how an oncogenic mutation affects immunosuppressive programmed death ligand 1 (PD-L1) expression may help in developing new therapeutic strategies. We show that oncogenic JAK2 (Janus kinase 2) activity caused STAT3 (signal transducer and activator of transcription 3) and STAT5 phosphorylation, which enhanced PD-L1 promoter activity and PD-L1 protein expression in JAK2^{V617F}-mutant cells, whereas blockade of JAK2 reduced PD-L1 expression in myeloid JAK2^{V617F}-mutant cells. PD-L1 expression was higher on primary cells isolated from patients with JAK2^{V617F}–myeloproliferative neoplasms (MPNs) compared to healthy individuals and declined upon JAK2 inhibition. JAK2^{V617F} mutational burden, pSTAT3, and PD-L1 expression were highest in primary MPN patient–derived monocytes, megakaryocytes, and platelets. PD-1 (programmed death receptor 1) inhibition prolonged survival in human MPN xenograft and primary murine MPN models. This effect was dependent on T cells. Mechanistically, PD-L1 surface expression in JAK2^{V617F}-mutant cells affected metabolism and cell cycle progression of T cells. In summary, we report that in MPN, constitutive JAK2/STAT3/STAT5 activation, mainly in monocytes, megakaryocytes, and platelets, caused PD-L1–mediated immune escape by reducing T cell activation, metabolic activity, and cell cycle progression. The susceptibility of JAK2^{V617F}-mutant MPN to PD-1 targeting paves the way for immunomodulatory approaches relying on PD-1 inhibition.

INTRODUCTION

Programmed death ligand 1 and 2 (PD-L1 and PD-L2) engage the programmed death receptor 1 (PD-1) on T cells and induce PD-1 signaling, which then causes multiple effects in T cells including exhaustion (*1*), alterations in glycolytic and mitochondrial metabolism (*2*), and reduced cell cycle activity (*3*). Tumor cells expressing PD-1 ligands on their surface use the PD-1 pathway to evade an effective antitumor immune response, and blockade of PD-1 is particularly effective in tumors with a high mutational burden (*4*). Genetic alterations including oncogenic activation of *Myc* (*5*) and loss of the tumor suppressor phosphatase and tensin homolog (*6*) cause increased PD-L1 expression (*7*).

JAK2 (Janus kinase 2) and *PD-L1* are both localized on chromosome 9p.24. In Hodgkin's lymphoma patients, transcription of the PD-L1 gene is increased upon amplification of chromosome 9p24.1 (*8*–*10*). It was initially unclear whether, comparable to the amplification of chromosome 9p24.1 causing higher JAK2 and PD-L1 copy numbers, oncogenic JAK2 activity can also induce PD-L1 expression and if so, whether this event is functionally causative for immune escape. A group of diseases characterized by oncogenic JAK2 activity

[1]Department of Hematology and Oncology, Medical Center, Faculty of Medicine, University of Freiburg, Freiburg 79106, Germany. [2]Faculty of Biology, Albert Ludwigs University of Freiburg, Freiburg 79104, Germany. [3]Institute of Surgical Pathology, Faculty of Medicine, University of Freiburg, Freiburg 79106, Germany. [4]Max Planck Institute for Immunobiology and Epigenetics, Freiburg 79108, Germany. [5]Department of Immunology, QIMR Berghofer Medical Research Institute, Brisbane, Queensland 4006, Australia. [6]School of Medicine, University of Queensland, Herston, Queensland 4006, Australia. [7]Institute of Molecular Medicine and Cell Research, Faculty of Medicine, University of Freiburg, Freiburg 79085, Germany. [8]German Cancer Consortium (DKTK) partner site Freiburg, Freiburg, Germany. [9]German Cancer Research Center (DKFZ), Heidelberg 69120, Germany. [10]Institute of Experimental Dermatology, Institute of Cardiogenetics, University of Lübeck, Lübeck 23562, Germany. [11]Berta-Ottenstein Programme, Faculty of Medicine, University of Freiburg, Freiburg 79106, Germany. [12]Department of Radiation Oncology, Faculty of Medicine, University of Freiburg, Freiburg 79106, Germany. [13]Department of Nuclear Medicine, Faculty of Medicine, University of Freiburg, Freiburg 79106, Germany. [14]Spemann Graduate School of Biology and Medicine, University of Freiburg, Freiburg 79085, Germany. [15]Center for Chronic Immunodeficiency, Medical Center, University of Freiburg, Freiburg 79106, Germany. [16]BIOSS Centre for Biological Signalling Studies, University of Freiburg, Freiburg 79104, Germany. [17]Internal Medicine II, Department of Hematology and Oncology, University Hospital of Jena, Jena 07745, Germany. [18]Leibniz Institute on Aging–Fritz Lipmann Institute, Jena 07745, Germany. [19]Department of Stem Cell Transplantation, University Medical Center Hamburg-Eppendorf, Hamburg 20246, Germany. [20]Unit of Experimental Hematology, San Raffaele Scientific Institute, and University of Vita-Salute San Raffaele, Milano 20132, Italy. [21]Royal Brisbane and Women's Hospital, Brisbane, Queensland, Australia. [22]University of Queensland, Herston, Queensland 4072, Australia. [23]Division of Blood and Marrow Transplantation, Department of Pediatrics, University of Minnesota, Minneapolis, MN 55455, USA.
*These authors contributed equally to this work.
†Corresponding author. Email: robert.zeiser@uniklinik-freiburg.de

are myeloproliferative neoplasms (MPNs). Most MPN patients carry an activating point mutation in the JAK2 kinase ($JAK2^{V617F}$).

Because MPNs are potentially immunogenic neoplasms, as demonstrated by their susceptibility to interferon α2b (IFN-α2b) (*11*) and detection of JAK2-specific T cells (*12*), we decided to clarify whether there is a role for PD-L1 in this type of disease. We found that $JAK2^{V617F}$ activity causes signal transducer and activator of transcription 3 (STAT3) and STAT5 phosphorylation, which in turn enhances PD-L1 promoter activity and increases PD-L1 protein expression. Both in murine MPN models and in primary patient samples, megakaryocytes, monocytes, and platelets expressed PD-L1 more abundantly compared to either wild-type (WT) littermates or healthy individuals. Consistent with the high PD-L1 expression observed, $JAK2^{V617F}$-MPN was susceptible to PD-1 blockade, which was dependent on T cells, in a $JAK2^{V617F}$-driven mouse model, in human MPN xenografts, and in an MPN patient who relapsed after allogeneic hematopoietic cell transplantation (allo-HCT). Mechanistically, $JAK2^{V617F}$-mutant cells affected metabolism and cell cycle progression in T cells via engagement with PD-L1–expressing mutant cells. Our findings identify a therapeutic concept for MPNs based on an oncogene-driven immune escape via the JAK2/STAT3/STAT5/PD-L1 axis.

RESULTS

JAK2 activation enhances PD-L1 expression via STAT3 phosphorylation

To test whether oncogenic JAK2 activity increases PD-L1 expression, we used a *Jak2*^{V617F} knock-in mouse model that develops polycythemia vera (*13*). In this model, we observed that PD-L1 surface expression was increased on megakaryocytes and monocytes derived from *Jak2*^{V617F} mice compared to *Jak2*-WT littermate control mice (Fig. 1, A and B, and fig. S1). PD-L1 expression also increased in primary murine bone marrow (BM) cells upon transfection with a $JAK2^{V617F}$ vector (Fig. 1C), indicating that JAK2 was responsible for the increase of PD-L1 surface expression in different cell types. The previously described four point one/ezrin/radixin/moesin (FERM) domain mutation (*14*), which causes oncogenic JAK2 activation ($JAK2^{FERM}$), also increased PD-L1 expression (Fig. 1D).

To understand the connection between oncogenic JAK2 and PD-L1, we transfected murine myeloid 32D cells with either a JAK2-WT vector or a $JAK2^{V617F}$ vector (*14*). 32D cells are erythropoietin-dependent (*15*) and have high endogenous PD-L1 expression. In the absence of erythropoietin, PD-L1 expression is lower, and under these conditions, PD-L1 expression increased in cells carrying the $JAK2^{V617F}$ mutation (Fig. 1, E and F). The same effects of mutant JAK2 on PD-L1 expression were seen in lymphoid Ba/F3 cells (fig. S2, A and B).

Treatment with the JAK1/2 inhibitor ruxolitinib reduced PD-L1 expression in $JAK2^{V617F}$-mutant 32D cells (Fig. 1, G and H) and Ba/F3 cells (fig. S2C). In contrast, when Ba/F3 cells contained a $JAK2^{V617F/L983F}$ mutation conferring ruxolitinib resistance, the PD-L1 expression declined less (fig. S2D). JAK2-specific inhibition with SD-1029 reduced PD-L1 expression in $JAK2^{V617F}$-mutant 32D (Fig. 1I) and Ba/F3 cells (fig. S2, E and F) in a dose-dependent manner, without major cytotoxic effects at the concentrations applied (fig. S2G).

To test our hypothesis that JAK2 activation enhances PD-L1 promoter activity via STAT phosphorylation, we analyzed phosphorylated STAT1 (pSTAT1), pSTAT3, and pSTAT5 in the presence of oncogenic $JAK2^{V617F}$. Active tyrosine pSTAT3 and pSTAT5 were increased in $JAK2^{V617F}$-mutant 32D cells compared to JAK2-WT 32D cells and, to a lesser extent, pSTAT1 also increased (Fig. 1, J and K). In agreement with this, pSTAT3 was higher in $JAK2^{V617F}$ Ba/F3 cells compared to empty-vector Ba/F3 cells (fig. S2, H to K).

Then, to understand which pathway is involved in promoting PD-L1 expression, we made use of vectors expressing STAT proteins with gain-of-function (GOF) or loss-of-function (LOF) mutations. The STAT3-activating mutation Y640F (*16*) increased the expression of PD-L1 on 32D cells compared to STAT3-WT vector (Fig. 1L). A similar pattern was observed in Ba/F3 cells with an activating STAT3 mutation (fig. S2L). Conversely, the STAT3 LOF mutations R382W and V637M reduced the expression of PD-L1 in $JAK2^{V617F}$-mutant 32D cells (Fig. 1M) and Ba/F3 cells (fig. S2M). Consistent with the idea that JAK2/STAT3 and PD-L1 are functionally connected, inhibition of STAT3 phosphorylation reduced PD-L1 expression (fig. S2N). In addition, a STAT5 GOF mutation (*17*) caused increased PD-L1 expression, although to a lesser extent than the STAT3 GOF mutation (Fig. 1L). Consistent with a role for STAT5, the inhibition of STAT5 phosphorylation slightly reduced PD-L1 expression in 32D cells (fig. S2O) and Ba/F3 cells (fig. S2P). A STAT1 GOF mutation had no significant effect on PD-L1 expression (Fig. 1L). Our data are consistent with findings by others showing that STAT3 and STAT5 can bind the PD-L1 promoter (*18*).

To evaluate the concept that JAK2 inhibition blocks immune responses in MPN, we analyzed the amount of serum IFN-γ in mice bearing a $JAK2^{V617F}$ MPN, which were treated with ruxolitinib or vehicle. We observed that ruxolitinib reduced IFN-γ (fig. S3). In light of these findings, it is likely that, although therapeutic JAK2 inhibition will render MPN more immunogenic on the basis of reduced PD-L1 expression, this intervention will at the same time counteract the T cell immune response against MPN.

In contrast to $JAK2^{V617F}$, other oncogenic mutations, including FLT3-ITD, FLT3-TKD, cKIT (D816V), epidermal growth factor receptor (Del19, L861Q, and L858R), or platelet-derived growth factor receptor (FIP1L1-PDGFRA), did not increase PD-L1 surface expression (fig. S4, A and B). Because some of these mutations are found in acute myeloid leukemia (AML) (*19*, *20*), we analyzed the BM of AML patients and found that AML cells were mostly PD-L1–negative (fig. S4, C and D). Consistently, pSTAT3 abundance was also low in primary human AML cells (fig. S4, E and F).

JAK2 activation enhances PD-L1 expression in human cells

To evaluate whether the data obtained in murine cells were also applicable to human cells, we studied JAK2-WT or $JAK2^{V617F}$ human cell lines. Transfection of K562 cells that express the ecotropic retrovirus receptor (*21*) with $JAK2^{V617F}$ increased PD-L1 expression compared to empty-vector cells (Fig. 2, A and B). PD-L1 expression decreased upon JAK2 inhibition (Fig. 2C). In addition, PD-L1 expression and pSTAT3 in different human $JAK2^{V617F}$ cell lines (UKE-1, SET-2, and MUTZ-8) could be reduced by specific JAK2 inhibition and ruxolitinib (Fig. 2, D to L). We tested the activity of the PD-L1 promoter using luciferase reporter assays (fig. S5) in K562 cells. The activity of the PD-L1 promoter was higher in $JAK2^{V617F}$-mutant K562 cells compared to empty-vector K562 cells (Fig. 2M). PD-L1 promoter activity declined upon JAK2 and STAT3 inhibition (Fig. 2, N and O).

In addition, we studied pSTAT1, pSTAT3, and pSTAT5 in K562 cells. We found that transfection of $JAK2^{V617F}$ increased pSTAT3 and pSTAT5, but not pSTAT1 in K562 cells compared to empty vector (fig. S6, A to C). A STAT1 GOF mutation did not increase PD-L1 expression in K562 cells, whereas PD-L1 increased in the presence of STAT3 GOF and STAT5 GOF mutations (fig. S6D).

Multiple cell types express increased PD-L1 in MPN patients

Next, we analyzed PD-L1 expression on different primary human cells in the peripheral blood (PB) of MPN patients (patients' characteristics are shown in table S1). PD-L1 expression on PB cells and platelets was higher in JAK2^{V617F} MPN patients compared to healthy volunteers (Fig. 3, A and B). We observed that T cells, monocytes, myeloid-derived

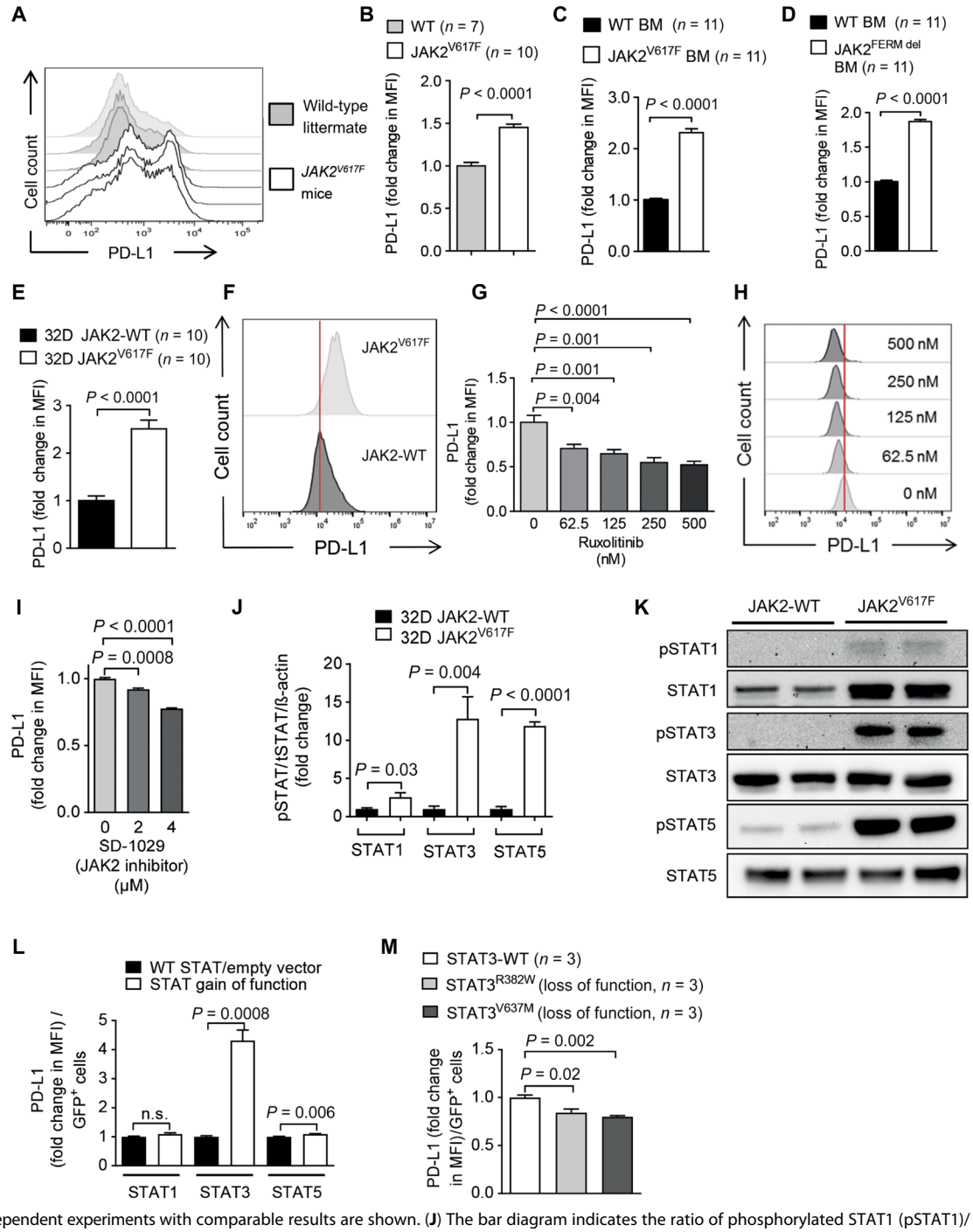

Fig. 1. JAK2^{V617F} activation increases PD-L1 expression in myeloid cells. (**A**) The representative histograms show the expression of programmed death ligand 1 (PD-L1) on CD41$^+$ platelets from the spleens of wild-type (WT) littermate mice (gray, $n = 3$) and JAK2^{V617F} mice (white, $n = 3$). One of three independent experiments is shown. (**B**) The bar diagrams show the fold change of PD-L1 expression on CD41$^+$ platelets isolated from the spleens of WT littermate and JAK2^{V617F} mice. Data are pooled from two independent experiments (WT littermate mice, $n = 7$; JAK2^{V617F} mice, $n = 10$). MFI, mean fluorescence intensity. (**C** and **D**) The bar diagrams show PD-L1 expression in murine primary BALB/c bone marrow (BM) cells isolated from mice on day 4 after treatment with 5-fluorouracil, after infection with either GFP$^+$JAK2^{V617F} virus (C) or GFP$^+$-JAK2 virus (deletion of the FERM inhibitory domain) (D). Data are pooled from 11 technical replicates. (**E**) The bar diagram shows PD-L1 expression on 32D cells expressing JAK2 wild type (JAK2-WT, black) or JAK2^{V617F} (white). Data are pooled from three independent experiments ($n = 10$ per group). (**F**) The representative histograms show PD-L1 expression on 32D JAK2-WT cells (dark gray) or 32D JAK2^{V617F} cells (light gray). (**G**) The bar diagram shows PD-L1 expression on 32D JAK2^{V617F} cells after exposure to ruxolitinib. Data are pooled from three independent experiments. (**H**) The representative histograms show PD-L1 expression on 32D JAK2^{V617F} cells after exposure to different concentrations of ruxolitinib. (**I**) The graph shows PD-L1 expression on 32D JAK2^{V617F} cells exposed to the specific JAK2 inhibitor SD-1029. Data ($n = 4$ per group) from one of three independent experiments with comparable results are shown. (**J**) The bar diagram indicates the ratio of phosphorylated STAT1 (pSTAT1)/STAT1/β-actin, pSTAT3/STAT3/β-actin, and pSTAT5/STAT5/β-actin for 32D JAK2-WT or JAK2^{V617F} cells. Pooled data ($n = 4$ per group) are from two independent experiments. (**K**) The Western blots display STAT1, STAT3, and STAT5 total protein and pSTAT1, pSTAT3, and pSTAT5 in 32D JAK2-WT or 32D JAK2^{V617F} cells. The blots are representative of two independent experiments. (**L**) The bar diagram displays the fold change of PD-L1 expression (flow cytometry) on 32D cells that were transfected with a vector containing STAT1 (R321G), STAT3 (Y640F), or STAT5 (S711F) with activating mutations (gain of function) or the respective WT STATs (for STAT1/STAT3) or empty vector (STAT5). One representative ($n = 3$ per group) of two independent experiments is displayed. (**M**) The bar diagram displays the fold change of PD-L1 expression (flow cytometry) on 32D^{V617F} cells that were transfected with a vector containing two different STAT3 loss-of-function mutations (R382W/V637M). Pooled data are from two independent experiments ($n = 3$ per group). n.s., not significant; tSTAT, total signal transducer and activator of transcription.

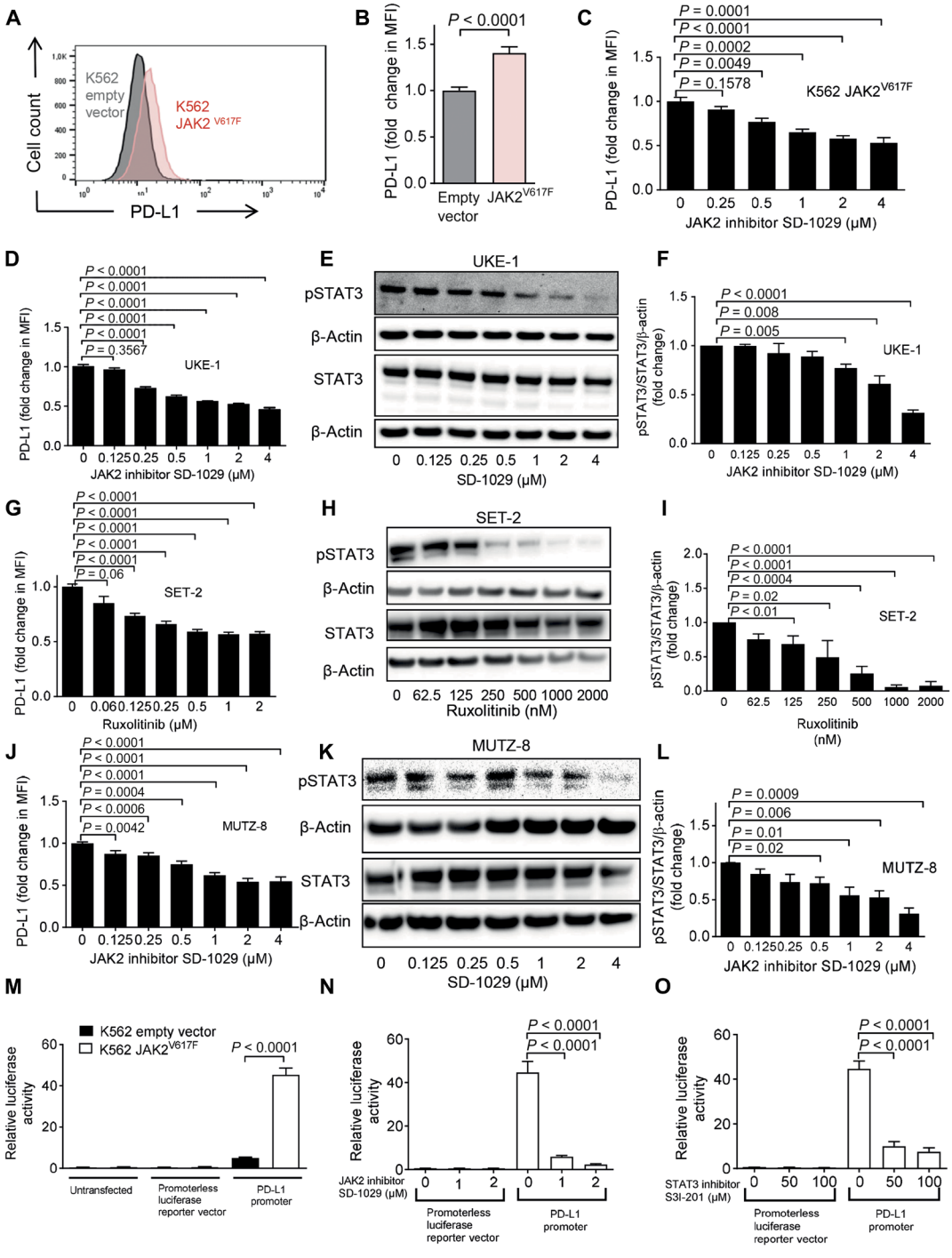

Fig. 2. The mutation JAK2^{V617F} promotes de novo PD-L1 gene transcription in human cells. (**A**) The histograms show the mean fluorescence intensity (MFI) for PD-L1 on K562 cells (transfected with empty vector or JAK2^{V617F} vector). One representative experiment of three experiments with a comparable pattern is shown. The analysis was done on GFP^{+} sorted cells within 3 days after transfection. (**B**) The bar diagram displays the fold change of PD-L1 expression (flow cytometry) on K562 cells transfected with empty vector or with JAK2^{V617F}. The data are pooled from four independent experiments ($n = 12$ per group). (**C**) The bar diagram displays the fold change of PD-L1 expression (flow cytometry) on K562 JAK2^{V617F} cells that were exposed to different concentrations of the JAK2 inhibitor SD-1029. Pooled data are from two independent experiments ($n = 6$ at each concentration). (**D**) The bar diagram displays the fold change of PD-L1 expression (flow cytometry) for the JAK2^{V617F}-positive cell line UKE-1 treated with the JAK2 inhibitor SD-1029 ($n = 7$ at each concentration). (**E**) The Western blots display STAT3 total protein, β-actin, and pSTAT3 in UKE-1 cells being treated with the JAK2 inhibitor SD-1029. The blots are representative of three independent experiments. (**F**) The bar diagram indicates the ratio of pSTAT3/STAT3/β-actin (normalized to 1 in the condition without JAK2 inhibitor) for the cells described in (E). Pooled data are from three replicates ($n = 3$ for each concentration). (**G**) The bar diagram displays the fold change of PD-L1 expression (flow cytometry) for the JAK2^{V617F}-positive cell line SET-2 treated with ruxolitinib. Pooled data are from three independent experiments (concentrations 0 to 0.5 μM, $n = 12$; concentrations 1 and 2 μM, $n = 6$). (**H**) The Western blots display STAT3, β-actin, and pSTAT3 in SET-2 cells being treated with ruxolitinib. The blots are representative of three independent experiments. (**I**) The bar diagram indicates the pSTAT3/STAT3/β-actin ratio for cells described in (H). Pooled data are from three independent experiments ($n = 3$ for each concentration). (**J**) The bar diagram displays the fold change of PD-L1 expression (flow cytometry) for the JAK2^{V617F}-positive cell line MUTZ-8 that was treated with the JAK2 inhibitor SD-1029 ($n = 3$ for each concentration). (**K**) The Western blots display STAT3 total protein, β-actin, and pSTAT3 in MUTZ-8 cells being treated with the JAK2 inhibitor SD-1029. The blots are representative of three independent experiments. (**L**) The bar diagram indicates the ratio of pSTAT3/STAT3/β-actin for cells described in (K). Pooled data are from three independent experiments ($n = 3$ for each concentration). (**M**) The bar diagram indicates the relative luminescence activity of K562 cells (containing empty vector or JAK2^{V617F}), which were left untransfected or transfected with either a promoterless luciferase reporter vector (pgl4.13) or a reporter vector containing the PD-L1 promoter. Pooled data are from three technical replicates ($n = 6$ for each condition). (**N**) The bar diagram indicates the relative luciferase activity of K562 JAK2^{V617F} cells transfected with either the promoterless luciferase reporter vector pgl4.13 or the reporter vector containing the PD-L1 promoter and treated with the JAK2 inhibitor SD-1029. Pooled data are from three independent experiments ($n = 6$ for each condition). (**O**) The bar diagram indicates the relative luminescence activity of K562 JAK2^{V617F} cells transfected with either the promoterless luciferase reporter vector pgl4.13 or the reporter vector containing the PD-L1 promoter and treated with the STAT3 inhibitor S3I-201. Pooled data are from three independent experiments ($n = 6$ for each condition).

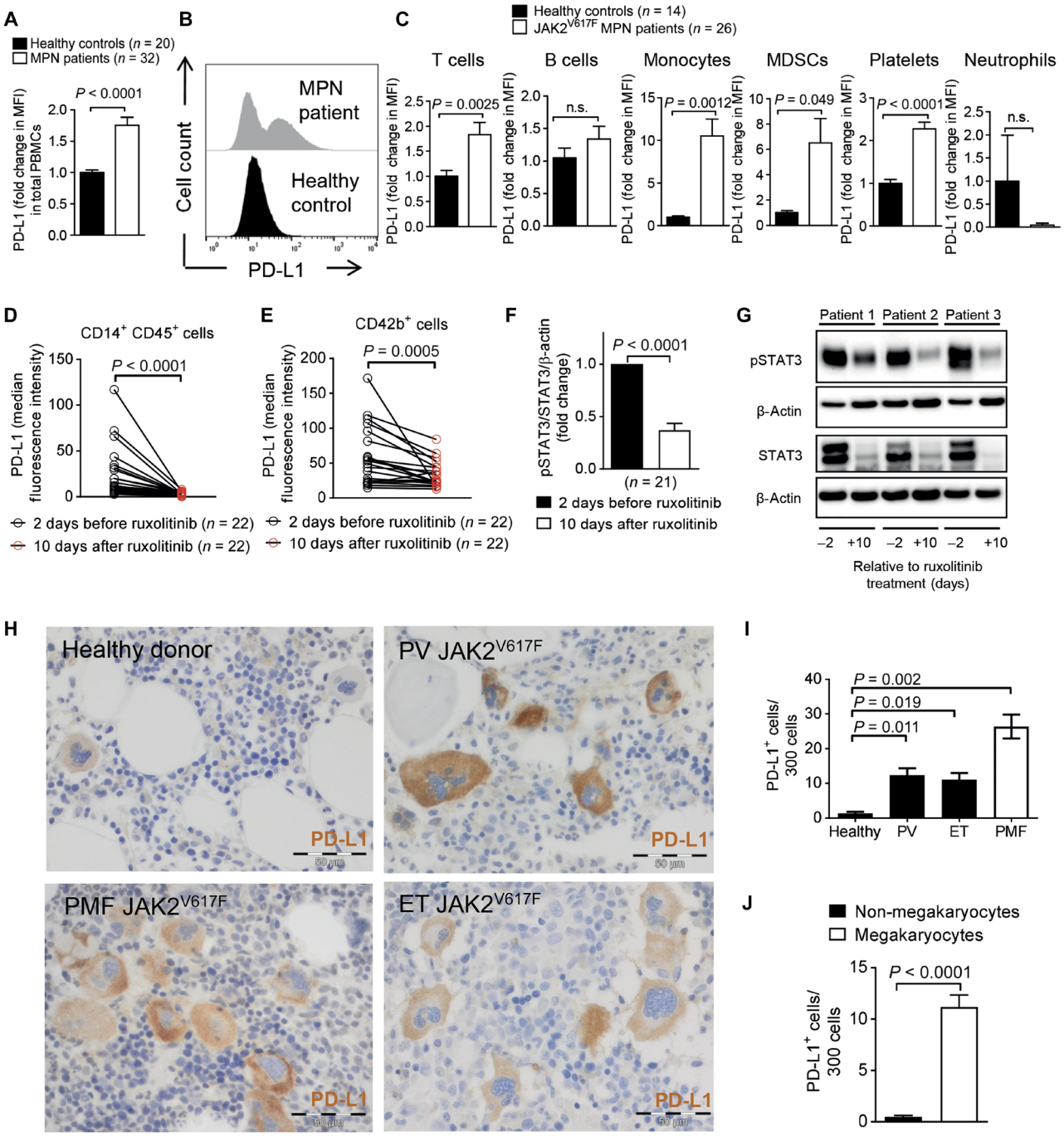

Fig. 3. PD-L1 is expressed on different cell types in MPN patients. (**A**) The bar diagram indicates the expression of PD-L1 on peripheral blood cells and platelets from healthy volunteers or myeloproliferative neoplasm (MPN) patients. (**B**) The histograms show PD-L1 expression on peripheral blood cells and platelets in healthy individuals or MPN patients as described in (A). (**C**) The bar diagrams show PD-L1 expression in different cell types: T cells ($CD3^+$), B cells ($CD19^+$), monocytes ($CD11b^+CD14^+$), myeloid-derived suppressor cells (MDSCs) ($CD11b^+CD33^+CD14^-$), platelets ($CD42b^+$), and neutrophils ($CD11b^+CD15^+$) from multiple MPN patients and healthy controls. Data were normalized to the PD-L1 MFI of healthy controls set as 1. (**D** and **E**) The diagrams show PD-L1 expression (MFI) in $CD14^+$ monocytes (D) and $CD42b^+$ platelets (E) from MPN patients on day 2 before ruxolitinib treatment and 10 days after start of ruxolitinib. Each data point indicates the measurement of an individual patient at the indicated time point. The *P* value was determined by using the Wilcoxon matched-pairs signed-rank test. (**F**) The bar diagram shows the pSTAT3/STAT3/β-actin ratio within peripheral blood mononuclear cells (PBMCs) from MPN patients on day 2 before ruxolitinib treatment and 10 days after start of ruxolitinib. Pooled results are from 21 patients. (**G**) The Western blots show pSTAT3 and STAT3 protein amounts within PBMCs from three representative MPN patients on day 2 before ruxolitinib treatment and 10 days after start of ruxolitinib. (**H**) Displayed are representative BM biopsies from a healthy control and different MPN patients with verified $JAK2^{V617F}$ mutations. $PD\text{-}L1^+$ cells appear in brown. Scale bar, 50 μm. (**I**) The bar diagram displays the number of $PD\text{-}L1^+$ cells out of 300 cells detected in BM biopsies from healthy volunteers or from multiple patients with the indicated MPN type. PV, polycythemia vera; ET, essential thrombocythemia; PMF, primary myelofibrosis. (**J**) The bar diagram displays the number of $PD\text{-}L1^+$ megakaryocytes versus all $PD\text{-}L1^+$ non-megakaryocyte cells detected out of 300 cells examined in BM biopsies of patients with JAK2-mutant MPN. Data are pooled from 39 patients.

suppressor cells (MDSCs), and platelets all had higher PD-L1 expression in MPN patients compared to healthy controls (Fig. 3C). The slight increase of PD-L1 in human T cells and B cells in MPN patients compared to healthy controls (Fig. 3C) is consistent with reports by others that B and T cells in some patients with MPN also carry the V617F mutation (*22*). The high expression of PD-L1 on MDSCs and the previous report that MPN is also associated with increased numbers of MDSCs (*23*) point to immunosuppressive potential of these cells in MPN. In contrast to JAK2^{V617F} peripheral blood mononuclear cells (PBMCs), calreticulin (CALR)–mutated PBMCs did not exhibit increased PD-L1 expression compared to cells derived from healthy individuals (fig. S7A). Cells with genomic amplification of JAK2 had increased PD-L1 expression (fig. S7B) and caused MPN-related death in a xenograft model, which could be prevented by anti–PD-1 therapy (fig. S7C).

Ruxolitinib treatment of MPN patients decreased PD-L1 expression on monocytes and platelets (Fig. 3, D and E). Compatible with a causal connection between JAK2 activation, STAT3 phosphorylation, and PD-L1 expression, pSTAT3/STAT3 ratios decreased upon ruxolitinib treatment (Fig. 3, F and G). Analysis of the BM from patients with different JAK2^{V617F} MPN entities and healthy BM donors showed that MPN patients had higher numbers of PD-L1$^+$ cells and that the most common cell type expressing PD-L1 was the megakaryocyte (Fig. 3, H to J).

Higher PD-L1 expression was associated with a more advanced MPN stage, as determined by histological signs and Dynamic International Prognostic Scoring System score (fig. S8, A to C) (*24*). MPN patients had lower CD4 and CD8 T cell numbers 5 years after diagnosis compared to MPN patients analyzed within the first year after diagnosis, suggesting that immunotherapy may be more effective in the earlier stages (fig. S8D).

We next transferred JAK2^{V617F}-transfected BM cells (BALB/c) into irradiated mice (BALB/c) and analyzed the distribution of PD-L1 in mice with JAK2^{V617F}-transfected BM that had developed MPN as evidenced by hematocrit and spleen size (fig. S9). Positron emission tomography (PET) combined with computed tomography (CT) imaging of mice with JAK2^{V617F}-transfected compared to WT BM using a ^{64}Cu-labeled anti–PD-L1 antibody showed the highest PD-L1 expression in the spleen (Fig. 4A), which is an organ with a high disease burden in this MPN model. Mice with JAK2^{V617F}-transfected BM had higher PD-L1 expression (PET signal) in spleen and BM compared to WT-BM mice (Fig. 4B). This result supports our previous in vitro findings and flow cytometry analysis with in vivo real-time data. Platelets had the highest PD-L1 expression in the JAK2^{V617F}-transfected BM MPN model (Fig. 4, C and D). To verify these results in an additional model, we used an MPN model that relies on conditional expression of a *JAK2^{V617F}* knock-in mutation in hematopoietic cells, activated via the Cre/lox system by crossing JAK2-L2 with Mx-Cre mice (JAK2-FLEX/+ or L2/+) (*25*). In this MPN model, we also observed that platelets had the highest expression of PD-L1 (Fig. 4, E and F).

To understand why monocytes, platelets, and megakaryocytes have the highest PD-L1 expression, we studied the JAK2^{V617F} allele burden in different cell types of MPN patients. We found that platelets and monocytes had a higher JAK2^{V617F} allele burden than B cells, T cells, or neutrophils from the same patients (Fig. 4G). We observed that human monocytes and platelets in the PB of MPN patients had higher pSTAT3 compared to B cells (CD19$^+$), T cells (CD3$^+$), or neutrophils (CD15$^+$) (Fig. 4, H and I).

MPNs are susceptible to PD-1 inhibition in the context of T cells

On the basis of the high PD-L1 expression of human MPN cells, we next tested our hypothesis that this disease is susceptible to therapeutic PD-1 inhibition. We transferred human PBMCs from three MPN patients who had relapsed after allo-HCT (patient characteristics are shown in table S2) into *RAG2$^{-/-}$Il2rg$^{-/-}$* mice and treated them with isotype immunoglobulin G (IgG) or anti-human PD-1–blocking antibody. *RAG2$^{-/-}$Il2rg$^{-/-}$* mice developed signs of MPN with increasing platelet counts (fig. S10A). We observed improved survival of mice treated with anti–PD-1 or anti–PD-L1 antibodies compared to mice treated with isotype IgG (Fig. 5, A to C). Consistent with improved survival, we observed lower numbers of human platelets and CD45$^+$ cells in the PB of mice treated with anti–PD-1 antibody compared to those of mice treated with isotype IgG (Fig. 5, D and E). In addition, we found reduced numbers of human CD45$^+$ cells in BM of mice treated with anti–PD-1 antibody compared to those of mice treated with isotype IgG (Fig. 5, F and G). Consistent with these findings, the JAK2^{V617F} allele burden was lower in mice treated with anti–PD-1 antibody than in mice treated with isotype IgG (Fig. 5H). Immunohistochemistry-based analysis of the BM did not show a significant difference in human CD45$^+$ cells in mice treated with anti–PD-1 antibody compared to the isotype IgG–treated group (Fig. 5, I and J).

The partial protection of mice treated with anti–PD-1 antibody compared to mice treated with isotype IgG was dependent on an intact donor T cell response, because depletion of CD3$^+$ T cells from the transferred PBMCs (fig. S10B) removed the survival advantage of mice treated with anti–PD-1 antibody compared to mice treated with isotype IgG (Fig. 5K). The graft-versus-host disease (GVHD) histopathology scores for *RAG2$^{-/-}$Il2rg$^{-/-}$* mice that had received human MPN cells and human T cells were not different for mice treated with anti–PD-1 antibody or isotype IgG (fig. S10C).

To extend these results from the human xenograft model to another MPN model, we used the JAK2^{V617F}-transfected syngeneic BM model. After full engraftment and development of MPN, defined by a hematocrit of more than 60% in the PB, the mice underwent antibody treatment. Survival of mice treated with anti-mouse PD-1 was improved compared to mice treated with isotype IgG (Fig. 5L). We observed that the ratio of effector/naive CD8$^+$ T cells increased in mice that were reconstituted with JAK2^{V617F}-transduced BM versus controls (Fig. 5M). This indicates that more effector T cells developed in these mice, which may have generated an anti-MPN effect. This effect was connected to PD-L1 expression because the ratio of effector/naive CD8$^+$ T cells increased further in mice treated with anti-mouse PD-L1 compared to mice treated with isotype IgG (Fig. 5M). Shannon diversity index of complementarity determining region 3 amino acid sequences for T cell receptor (TCR) α chains was significantly ($P = 0.04$) lower in T cells of anti–PD-1–treated mice (Fig. 5, N and O). These observations are in line with previous studies showing that T cell–mediated anti-leukemia response is linked to low TCR repertoire diversity (*26*).

PD-L1–expressing JAK2^{V617F}-mutant cells affect cell cycle progression and metabolism in T cells

When T cells were exposed to JAK2^{V617F} myeloid 32D cells, unbiased gene expression analysis revealed a down-regulation of multiple gene sets that represent metabolic pathways (Fig. 6A). One of the gene sets with reduced expression in T cells exposed to JAK2^{V617F} myeloid 32D cells was amino acid metabolism (Fig. 6A, asterisk). In agreement

with this finding, murine T cells exposed to JAK2^{V617F} Ba/F3 cells showed a down-regulation of genes related to methionine and cysteine metabolism, which are critical for T cell activation (fig. S11A) (*27*–*29*). The alanine serine and cysteine transporter system SLC1A5 (ASCT2), which was down-regulated in T cells upon exposure to JAK2^{V617F} Ba/F3 cells, is essential for T cell activation (*30*). Expression

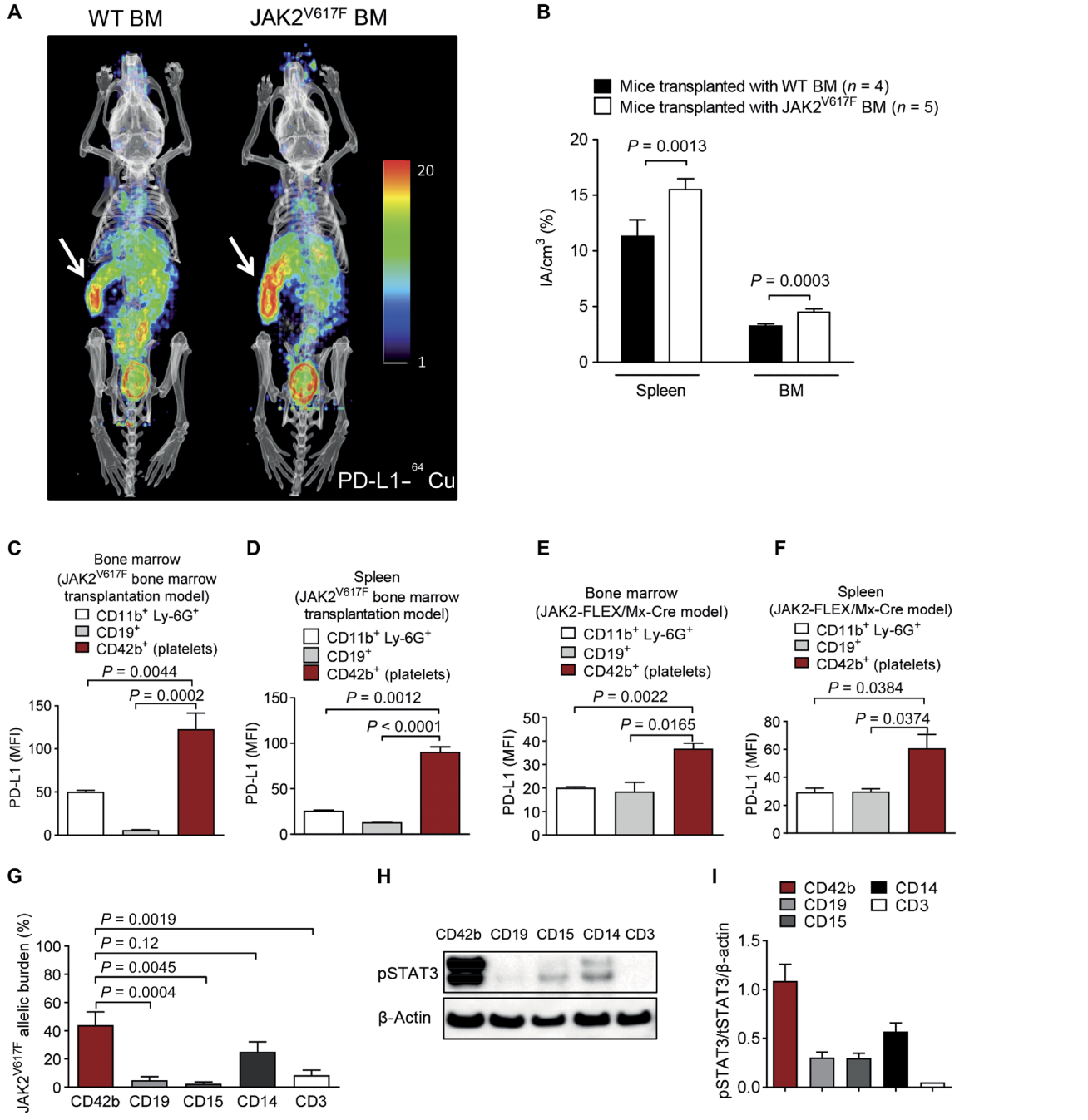

Fig. 4. PD-L1 expression is found in the spleen and the BM of mice transplanted with JAK2^{V617F}-transduced bone marrow. (**A**) Two representative mice imaged by positron emission tomography/computed tomography using a ^{64}Cu-labeled anti–PD-L1 antibody are shown. BALB/c mice had received either JAK2^{V617F}-transfected (right) or WT syngeneic BM (left) after total body irradiation (TBI, 6.5 grays). The signal intensity indicates areas with high PD-L1 expression. Arrows point toward the spleen (high signal intensity). The image is representative of four mice per group with comparable signal patterns. (**B**) The bar diagram shows the signal intensity in the indicated organs of mice transplanted as described in (A). Data are pooled from four or five mice per group. (**C** and **D**) The bar diagram shows the MFI for PD-L1 on different cells and platelets in the BM (C) or spleen (D) of mice transplanted as described in (A). $n = 5$ per group. (**E** and **F**) The bar diagram shows the MFI for PD-L1 on different cells and platelets in BM (E) and spleen (F) of JAK2-FLEX/Mx-Cre mice ($n = 3$ per group). (**G**) The bar diagram shows the JAK2^{V617F} allele burden in different cell populations isolated by cell sorting from 15 MPN patients. The JAK2^{V617F} allele burden was determined by quantitative polymerase chain reaction ($n = 15$ per group). (**H**) The Western blot shows the amounts of pSTAT3 and STAT3 in different cell populations isolated by cell sorting from a representative polycythemia vera patient. (**I**) The bar diagram shows the ratios of pSTAT3/STAT3/β-actin in different cell populations isolated by cell sorting from multiple MPN patients ($n = 5$ for CD42b, CD19, CD15, and CD3; $n = 3$ for CD14). IA, injected activity.

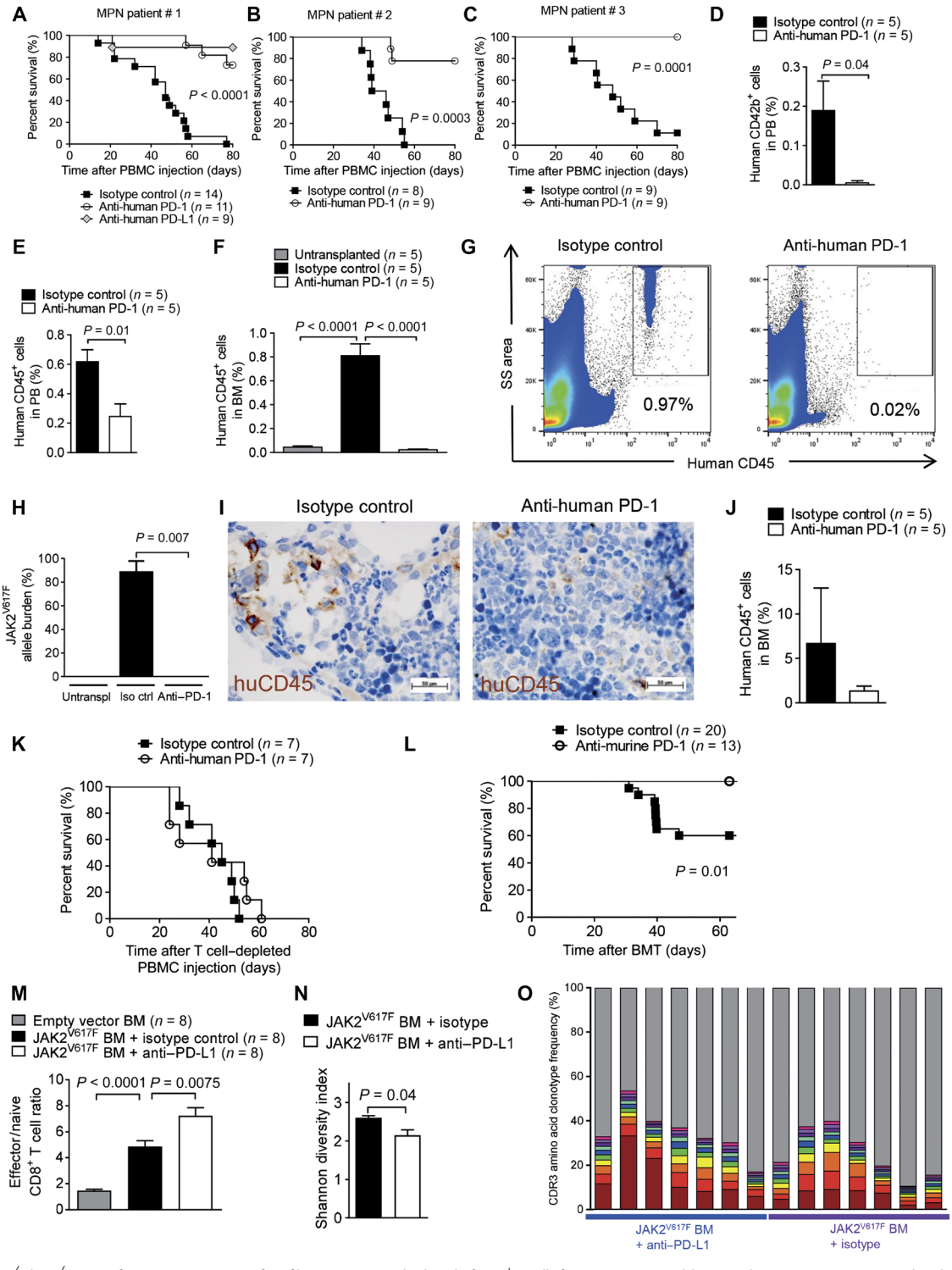

Fig. 5. PD-1 blockade improves survival in MPN mouse models. (**A** to **C**) The survival of *RAG2*$^{-/-}$*Il2rg*$^{-/-}$ mice after intravenous transfer of human PBMCs from patient #1 (A), patient #2 (B), and patient #3 (C) (table S2) is shown. Mice were treated with 250 μg of isotype control (Iso ctrl) antibody, anti-human programmed death receptor 1 (PD-1) antibody, or anti-human PD-L1 antibody on day 8 after PBMC injection. Pooled data are from three independent experiments. (**D** and **E**) The bar diagram shows the percentage of human CD42b$^+$ platelets (**D**) or human CD45$^+$ cells (**E**) in the peripheral blood (PB) of *RAG2*$^{-/-}$*Il2rg*$^{-/-}$ mice transplanted with PBMCs from MPN patient #1. The analysis was performed on day 21 after intravenous transfer of human PBMCs. (**F**) The bar diagram shows the percentage of human CD45$^+$ cells determined by flow cytometry in the BM of untreated *RAG2*$^{-/-}$*Il2rg*$^{-/-}$ mice. *RAG2*$^{-/-}$*Il2rg*$^{-/-}$ mice had received intravenous transfer of human PBMCs from patient #1 (table S2) and were treated with isotype antibody or anti-human PD-1 (250 μg, day 8). The analysis was performed on day 39 after intravenous transfer of human PBMCs. (**G**) Representative fluorescence-activated cell sorting plots showing the percentage of human CD45$^+$ cells in BM of *RAG2*$^{-/-}$*Il2rg*$^{-/-}$ mice transplanted and treated as described in (F). (**H**) The bar diagram shows the JAK2^{V617F} allele burden in BM harvested from *RAG2*$^{-/-}$*Il2rg*$^{-/-}$ mice treated as described in (F). (**I**) Representative pictures of human CD45$^+$ cells (brown) in the BM harvested from *RAG2*$^{-/-}$*Il2rg*$^{-/-}$ mice treated as described in (F). Scale bar, 50 μm. (**J**) Shown is the quantification of the CD45$^+$ cells in BM harvested from *RAG2*$^{-/-}$*Il2rg*$^{-/-}$ mice treated as described in (F). (**K**) Survival of *RAG2*$^{-/-}$*Il2rg*$^{-/-}$ mice after intravenous transfer of human PBMCs depleted of CD3$^+$ T cells from patient #1 (table S2) is shown. Mice were treated with isotype control or anti-human PD-1 (250 μg) on day 8 after transplantation. Data are pooled from two independent experiments. (**L**) Survival of BALB/c mice, which had received JAK2^{V617F}-transfected syngeneic BM after TBI and isotype control antibody or anti–PD-1 antibody. Data are pooled from two independent experiments. (**M**) The bar diagrams show the ratio of effector/naive CD8$^+$ T cells in spleens isolated from mice described in (L) on day 19 after transplantation ($n = 8$ per group). (**N**) The mean diversity index of T cell receptor α (TCRα) complementarity determining region 3 (CDR3) amino acid sequences for isotype control antibody or anti–PD-1 antibody groups is shown. Error bars represent SEM. (**O**) The abundance of the CDR3 amino acid clonotype frequency of the 10 strongest clones according to variable TCRαβ genes for isotype control antibody or anti–PD-1 antibody groups is shown. Each bar represents an individual mouse; different colors display different clones. Untranspl., untransplanted; SS, side scatter; BMT, bone marrow transplantation.

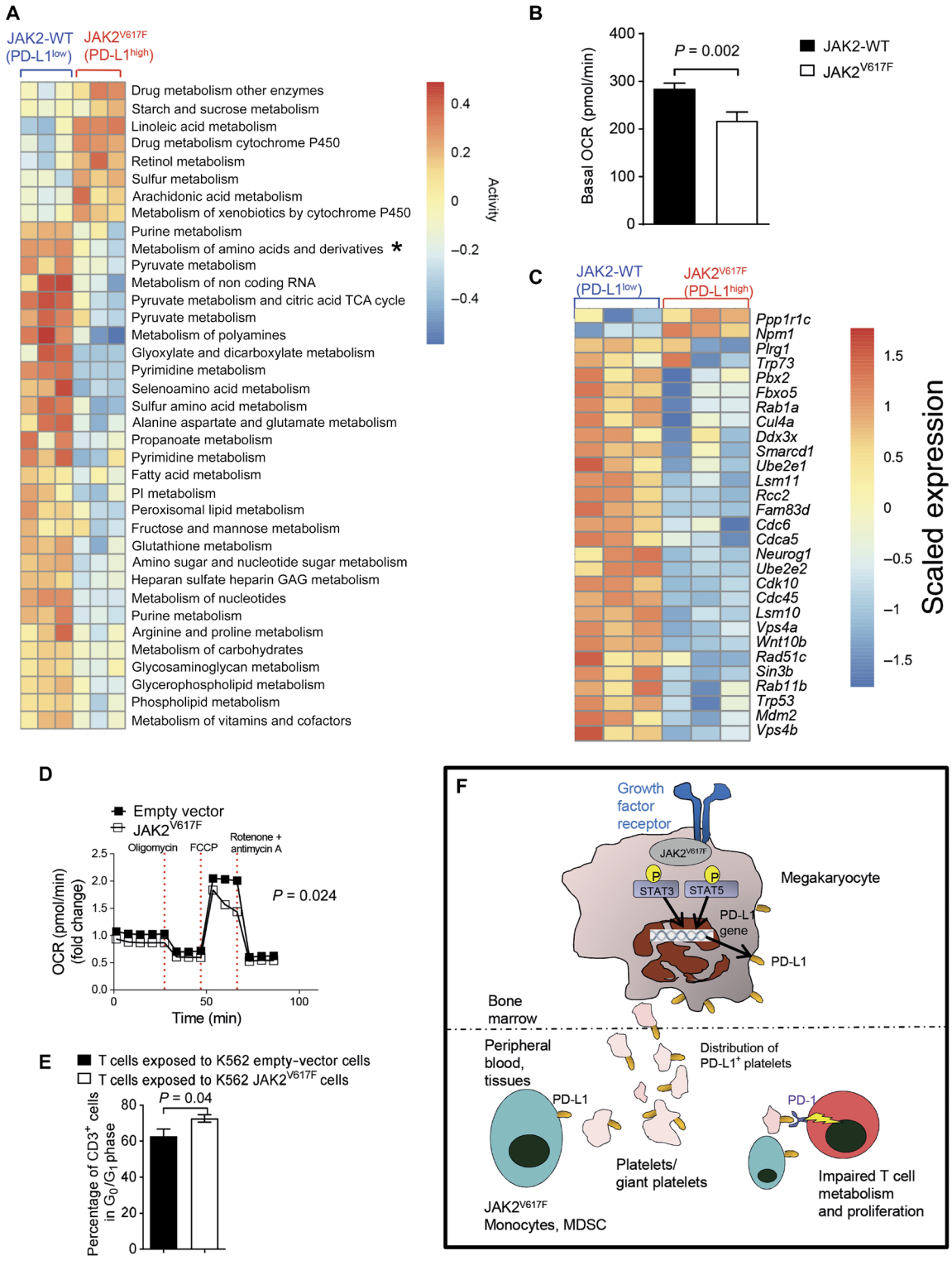

Fig. 6. JAK2^{V617F}-mutant cells affect metabolism and cell cycle in T cells. (**A**) The heat map depicts the activity scores of differentially regulated metabolic pathways in T cells (C3H) that were exposed to JAK2^{V617F}-mutant or JAK2-WT 32D cells (C3H) for 24 hours (n = 3 empty vector, n = 3 JAK2^{V617F}-mutant 32D cells). The asterisk indicates the metabolism of amino acids and derivatives for this metabolic pathway for which the groups are significantly different (adjusted P < 0.005). Pathways were selected from Kyoto Encyclopedia of Genes and Genomes and Reactome gene sets containing the word "Metabolism." (**B**) Basal oxygen consumption rate (OCR) of mouse CD3$^+$ T cells (C3H) that were exposed to 32D JAK2^{V617F} or 32D JAK2-WT cells (C3H) for 24 hours. Data were combined from three independent biological repeats. (**C**) The heat map depicts genes from the Gene Ontology term "Positive regulation of cell cycle phase transition" that have an absolute $\log_2$ fold change of >0.1 between T cells (C3H) that were exposed to JAK2^{V617F}-mutant or JAK2-WT 32D cells (C3H) for 24 hours (n = 3 JAK2-WT and n = 3 JAK2^{V617F}-mutant 32D cells). (**D**) Time course for OCR of human CD3$^+$ T cells that were exposed to human K562 cells with a JAK2^{V617F} mutation (or K562 cells with empty vector) for 24 hours at baseline and after oligomycin, carbonyl cyanide p-trifluoromethoxyphenylhydrazone (FCCP), and rotenone plus antimycin A exposure. Data were combined from two experiments. (**E**) The bar diagram represents the percentage of human CD3$^+$ cells that were in G_0/G_1 phase (noncycling) when T cells were exposed for 24 hours to K562 JAK2^{V617F} cells (or K562 cells with empty vector). The data are pooled from two independent experiments (n = 10 per group). (**F**) Proposed mechanism of the JAK2-mediated immune escape in MPN: Greater JAK2 activity increases STAT3 and STAT5 phosphorylation. pSTAT3 and pSTAT5 bind to and activate the PD-L1 promoter, resulting in PD-L1 transcription and consequently higher PD-L1 surface expression. Platelets derived from neoplastic (JAK2^{V617F}) megakaryocytes, as well as monocytes and MDSCs, all express PD-L1 abundantly and are distributed via the peripheral blood, which causes T cell exhaustion via interaction of PD-L1 on the platelets and myeloid cells with PD-1 on T cells.

of SLC1A5 on T cells declined in a cell dose-dependent manner when they were exposed to JAK2^{V617F} Ba/F3 cells (fig. S11B). Consistent with our findings, a functional link between amino acid metabolism and PD-1 activation has been reported (*2*).

To understand whether mutant JAK2–induced PD-L1 expression had an impact on T cell metabolism, we determined the rates of oxidative phosphorylation in CD3$^+$ T cells by measuring the oxygen consumption rate (OCR) at baseline and during a mitochondrial fitness test (*31*). Basal OCR in mouse CD3$^+$ T cells was decreased after exposure to JAK2^{V617F} 32D cells (Fig. 6B) or JAK2^{V617F} Ba/F3 cells (fig. S11, C and D). Previous reports had shown that aerobic glycolysis is a hallmark of effector lymphocyte metabolism (*31*), which was reduced in the T cells exposed to the JAK2^{V617F} 32D and JAK2^{V617F} Ba/F3 cells (Fig. 6B and fig. S11, C and D). Because cell cycle progression is affected by PD-1 ligation on T cells, we next analyzed cell cycle–related genes. We observed that gene sets relevant for G_1- to S-phase transition were down-regulated in mouse T cells (isolated from C3H mice) that were exposed to JAK2^{V617F} 32D (C3H background) cells (Fig. 6C). Cyclin-dependent kinase 6 (CDK6), which is required for cell cycle progression in T cells, was down-regulated in T cells exposed to JAK2^{V617F} Ba/F3 cells analyzed by gene expression array (fig. S11E). The gene expression of *Cdk8* was also down-regulated in T cells when JAK2^{V617F} Ba/F3 cells were present (fig. S11E). Conversely, gene expression of cyclin G2 (*Ccng2*), which induces cell cycle arrest, and cyclin-dependent kinase inhibitor 2D (*Cdkn2d*), which reduces cell cycle activity, was up-regulated in T cells exposed to JAK2^{V617F} Ba/F3 cells (fig. S11F). Consistently, we observed that the percentage of T cells in G_0/G_1 phase increased when T cells were exposed to JAK2^{V617F} Ba/F3 cells (fig. S11G). This pattern was not observed when the T cells were PD-1–deficient (fig. S11G), indicating that the effect was mediated via PD-1.

To understand whether these findings could be reproduced in human cells, we cocultured human T cells from healthy donors with JAK2^{V617F}K562 cells. Respiration in human CD3$^+$ T cells was decreased after exposure to JAK2^{V617F}K562 cells (Fig. 6D). In addition, the percentage of T cells in G_0/G_1 phase increased when T cells were exposed to JAK2^{V617F}K562 cells (Fig. 6E).

On the basis of our findings in the mouse model, we treated patient #1 (table S2), who was initially diagnosed with polycythemia vera. He had undergone allo-HCT, relapsed, and was resistant to multiple salvage therapies (ruxolitinib, hydroxyurea, and decitabine). The anti–PD-1 antibody nivolumab was used as an individualized approach. At the start of treatment, 98% of the CD3$^+$ cells were donor-derived, whereas 50% of the CD34$^+$ cells were recipient-derived (fig. S12A). Immunohistochemistry of the BM showed the underlying MPN with a transformation into AML at the time of relapse. No additional mutations (besides JAK2^{V617F}) in the PBMCs were found by using a 48-gene myeloid panel sequencing approach that was confirmed by whole-exome sequencing. In agreement with the findings in mice, in a patient with polycythemia vera we observed that recipient chimerism, JAK2^{V617F} allele burden, CD34$^+$ cells in the PB, and cellularity in the BM all decreased after nivolumab treatment (fig. S12, A to G). Conversely, the number of total CD3$^+$ cells in the PB increased after application of nivolumab (fig. S12, H and I).

On the basis of our findings, we propose a scenario where oncogenic JAK2 activity results in STAT3 and STAT5 phosphorylation, which in turn enhances PD-L1 promoter activity (Fig. 6G). The cells carrying JAK2^{V617F} express PD-L1 and thereby inhibit amino acid and glucose metabolism and cell cycle progression–promoting genes in T cells.

DISCUSSION

Once a cell has acquired an oncogenic mutation allowing for uncontrolled proliferation and avoidance of apoptosis, a critical next step in the development toward neoplastic disease is to escape the immune system. Because both events, oncogenic transformation and immune escape, have to occur at the beginning of neoplastic development, it is likely that certain oncogenic mutations cooperate with mechanisms that allow immune escape. We found that oncogenic JAK2 activation results in high expression of PD-L1, mainly on the surface of monocytes, MDSCs, megakaryocytes, and platelets, and that this is mediated via the JAK2-STAT3 and JAK2-STAT5 axes. Consistent with our findings, others showed that pSTAT3 binds to and activates the PD-L1 gene promoter (*32*, *33*). Because JAK2 is a canonical STAT3 activator and STAT3 activates PD-L1 transcription, the induction of PD-L1 in MPN was likely, and our study shows this connection experimentally in a systematic analysis of JAK2^{V617F}-mutant cells. Recently, a binding site for STAT5 was found in the *PD-L1* promoter region (*18*), but no functional connection between STAT5 activation and PD-L1 expression had been reported to date. We observed a minor role for STAT5 in PD-L1 expression, which was less prominent compared to the role of STAT3.

A limitation of the study is that we cannot clarify why AMLs do not exhibit high expression of PD-L1. A possible explanation is that other regulatory mechanisms for PD-L1 are active in AMLs. Interference with CMTM6 expression results in impaired PD-L1 protein expression because CMTM6 prevents PD-L1 from being targeted for lysosome-mediated degradation (*34*, *35*). Therefore, cells with a low amount of CMTM6 will have more PD-L1 degradation even if STAT3 activation is present. Another limitation of our study is that we used xenograft models of MPN, which are artificial because the recipient mice are immunodeficient. To correct for this, we had transferred T cells along with the MPN cells to allow for immune-mediated effects. An additional limitation is that our findings can only be applied to JAK2^{V617F}-mutant MPN, and we did not clarify which immune escape mechanisms are active in JAK2-negative MPN.

For a variety of tumor entities such as non–small cell lung cancer (*36*) and Hodgkin's lymphoma (*9*), high expression of PD-L1 favors sensitivity of the malignancy to PD-1 inhibition. In particular, increased expression of PD-L1 on hematopoietic cells was associated with increased response (*37*). This is consistent with our finding showing that PD-L1 expression on cells was high in MPN, which then responded to PD-1 inhibition in an allo-HCT patient who had relapsed after transplant. Previous work had shown that T cell–mediated immunosurveillance plays a central role in MPN progression, because T cells recognizing mutant JAK2 can be found in MPN patients (*12*), and MPNs are immunogenic because they respond to IFN-α2b (*11*).

Our observation that PD-L1 expression is high on megakaryocytes is consistent with previous reports indicating that this cell type is an important disease-driving force in MPN (*38*, *39*). However, other cell types, such as monocytes, MDSCs, and lymphocytes, expressed PD-L1, which is consistent with the fact that these cells also have a certain JAK2^{V617F} allele burden (*22*). When murine or human T cells were exposed to PD-L1^{high} cells with mutant JAK2, we observed major changes in metabolism, senescence, IFN-γ production, and cell cycle activity. In particular, cysteine metabolism was reduced when murine T cells were exposed to PD-L1^{high} JAK2^{V617F} cells. This may be a major mechanism for JAK2^{V617F} cells to affect T cell activation because cysteine is the limiting precursor for glutathione synthesis, a prerequisite for antigen-dependent proliferation of T cells (*29*). The decreased

OCR we observed in T cells exposed to JAK2^{V617F} cells indicates that these T cells were overall less metabolically active, which is consistent with the idea that there is decreased cell cycle activity in this T cell population. Reduced proliferative capacity due to cell cycle inhibition may contribute to the reduced antitumor activity of T cells exposed to PD-L1^{high} JAK2^{V617F} cells. DNA methyltransferase inhibitor treatment can also up-regulate PD-L1 expression in MDS, possibly causing disease resistance (*40*). Checkpoint inhibition can induce response rates above 50%, as recently reported for patients with different hematologic malignancies treated with an anti–CTLA-4 antibody after allo-HCT (*41*). We showed that activation of the JAK2/STAT3 and JAK2/STAT5 axes causes PD-L1–mediated immune escape in MPN. We defined megakaryocytes, platelets, and monocytes as the cell populations with the highest PD-L1 expression and characterized a gene signature in T cells that were affected by the PD-L1–expressing cells. Furthermore, we reported the susceptibility of MPN to PD-1 inhibition, which should serve as a basis for immunotherapeutic approaches that rely on PD-1 inhibition in this disease entity.

MATERIALS AND METHODS

Study design

For the sample size in the murine survival experiments, a power analysis was performed. A sample size of at least $n = 8$ per group was determined to reach a statistical significance of 0.05 to detect an effect size of at least 1.06 with 80% power. Mice were assigned randomly to the experimental groups. All samples and mice were included in our analysis. Experiments were performed in a nonblinded fashion, except for the blinded GVHD severity scoring.

Human subjects

Human sample collection and analysis were approved by the ethics committee of the University of Freiburg, Germany (protocol numbers 10024/13 and 558/15). Blood was collected from MPN patients or healthy volunteers after informed consent.

Statistical analysis

GraphPad Prism v5.03 was used for statistical analysis. Normally distributed data were analyzed using the unpaired two-tailed *t* test. When the data did not conform to a normal distribution, the Mann-Whitney *U* test was used. Differences in mouse survival (Kaplan-Meier survival curves) were analyzed by log-rank test. Data are presented as means and SEM, unless otherwise indicated. $P < 0.05$ was considered to be statistically significant.

SUPPLEMENTARY MATERIALS

www.sciencetranslationalmedicine.org/cgi/content/full/10/429/eaam7729/DC1
Materials and Methods
Fig. S1. PD-L1 expression is increased in JAK2^{V617F} primary mouse monocytes compared to WT mouse monocytes.
Fig. S2. Oncogenic JAK2^{V617F} increases PD-L1 expression.
Fig. S3. Ruxolitinib treatment reduces serum IFN-γ in mice transplanted with JAK2^{V617F}-transduced BM.
Fig. S4. PD-L1 expression is not affected by different activating mutations.
Fig. S5. The luciferase reporter assay vector maps are displayed.
Fig. S6. STAT3 and STAT5 activation increase PD-L1 expression.
Fig. S7. PD-L1 expression increases in human JAK2^{V617F}-mutant cells.
Fig. S8. PD-L1 expression depends on the MPN disease stage.
Fig. S9. Transfer of JAK2^{V617F}-mutant BM results in MPN features.
Fig. S10. Anti–PD-1 treatment does not increase GVHD scores.
Fig. S11. JAK2^{V617F}-mutant Ba/F3 cells affect T cell metabolism and cell cycle.
Fig. S12. Anti–PD-1 treatment decreases disease burden of an MPN patient.
Table S1. JAK2^{V617F} MPN patients' characteristics.
Table S2. MPN patients for xenograft experiments.
Table S3. Antibodies.
Table S4. Primer sequences (promoter assay).
Table S5. Primer sequences (STAT1 mutagenesis).

REFERENCES AND NOTES

1. F. Tsushima, S. Yao, T. Shin, A. Flies, S. Flies, H. Xu, K. Tamada, D. M. Pardoll, L. Chen, Interaction between B7-H1 and PD-1 determines initiation and reversal of T-cell anergy. *Blood* **110**, 180–185 (2007).
2. N. Patsoukis, K. Bardhan, P. Chatterjee, D. Sari, B. Liu, L. N. Bell, E. D. Karoly, G. J. Freeman, V. Petkova, P. Seth, L. Li, V. A. Boussiotis, PD-1 alters T-cell metabolic reprogramming by inhibiting glycolysis and promoting lipolysis and fatty acid oxidation. *Nat. Commun.* **6**, 6692 (2015).
3. Y. Latchman, C. R. Wood, T. Chernova, D. Chaudhary, M. Borde, I. Chernova, Y. Iwai, A. J. Long, J. A. Brown, R. Nunes, E. A. Greenfield, K. Bourque, V. A. Boussiotis, L. L. Carter, B. M. Carreno, N. Malenkovich, H. Nishimura, T. Okazaki, T. Honjo, A. H. Sharpe, G. J. Freeman, PD-L2 is a second ligand for PD-1 and inhibits T cell activation. *Nat. Immunol.* **3**, 261–268 (2001).
4. N. McGranahan, A. J. Furness, R. Rosenthal, S. Ramskov, R. Lyngaa, S. K. Saini, M. Jamal-Hanjani, G. A. Wilson, N. J. Birkbak, C. T. Hiley, T. B. Watkins, S. Shafi, N. Murugaesu, R. Mitter, A. U. Akarca, J. Linares, T. Marafioti, J. Y. Henry, E. M. Van Allen, D. Miao, B. Schilling, D. Schadendorf, L. A. Garraway, V. Makarov, N. A. Rizvi, A. Snyder, M. D. Hellmann, T. Merghoub, J. D. Wolchok, S. A. Shukla, C. J. Wu, K. S. Peggs, T. A. Chan, S. R. Hadrup, S. A. Quezada, C. Swanton, Clonal neoantigens elicit T cell immunoreactivity and sensitivity to immune checkpoint blockade. *Science* **351**, 1463–1469 (2016).
5. S. C. Casey, L. Tong, Y. Li, R. Do, S. Walz, K. N. Fitzgerald, A. M. Gouw, V. Baylot, I. Gütgemann, M. Eilers, D. W. Felsher, MYC regulates the antitumor immune response through CD47 and PD-L1. *Science* **352**, 227–231 (2016).
6. A. T. Parsa, J. S. Waldron, A. Panner, C. A. Crane, I. F. Parney, J. J. Barry, K. E. Cachola, J. C. Murray, T. Tihan, M. C. Jensen, P. S. Mischel, D. Stokoe, R. O. Pieper, Loss of tumor suppressor PTEN function increases B7-H1 expression and immunoresistance in glioma. *Nat. Med.* **13**, 84–88. (2007).
7. K. Kataoka, Y. Shiraishi, Y. Takeda, S. Sakata, M. Matsumoto, S. Nagano, T. Maeda, Y. Nagata, A. Kitanaka, S. Mizuno, H. Tanaka, K. Chiba, S. Ito, Y. Watatani, N. Kakiuchi, H. Suzuki, T. Yoshizato, K. Yoshida, M. Sanada, H. Itonaga, Y. Imaizumi, Y. Totoki, W. Munakata, H. Nakamura, N. Hama, K. Shide, Y. Kubuki, T. Hidaka, T. Kameda, K. Masuda, N. Minato, K. Kashiwase, K. Izutsu, A. Takaori-Kondo, Y. Miyazaki, S. Takahashi, T. Shibata, H. Kawamoto, Y. Akatsuka, K. Shimoda, K. Takeuchi, T. Seya, S. Miyano, S. Ogawa, Aberrant PD-L1 expression through 3′-UTR disruption in multiple cancers. *Nature* **534**, 402–406 (2016).
8. M. R. Green, S. Monti, S. J. Rodig, P. Juszczynski, T. Currie, E. O'Donnell, B. Chapuy, K. Takeyama, D. Neuberg, T. R. Golub, J. L. Kutok, M. A. Shipp, Integrative analysis reveals selective 9p24.1 amplification, increased PD-1 ligand expression, and further induction via JAK2 in nodular sclerosing Hodgkin lymphoma and primary mediastinal large B-cell lymphoma. *Blood* **116**, 3268–3277 (2010).
9. S. M. Ansell, A. M. Lesokhin, I. Borrello, A. Halwani, E. C. Scott, M. Gutierrez, S. J. Schuster, M. M. Millenson, D. Cattry, G. J. Freeman, S. J. Rodig, B. Chapuy, A. H. Ligon, L. Zhu, J. F. Grosso, S. Young Kim, J. M. Timmerman, M. A. Shipp, P. Armand, PD-1 blockade with nivolumab in relapsed or refractory Hodgkin's lymphoma. *N. Engl. J. Med.* **372**, 311–319 (2015).
10. M. G. Roemer, R. H. Advani, A. H. Ligon, Y. Natkunam, R. A. Redd, H. Homer, C. F. Connelly, H. H. Sun, S. E. Daadi, G. J. Freeman, P. Armand, B. Chapuy, D. de Jong, R. T. Hoppe, D. S. Neuberg, S. J. Rodig, M. A. Shipp, *PD-L1* and *PD-L2* genetic alterations define classical Hodgkin lymphoma and predict outcome. *J. Clin. Oncol.* **34**, 2690–2697 (2016).
11. A. Tichelli, A. Gratwohl, C. Berger, A. Lori, A. Würsch, A. Dieterle, C. Thomssen, C. Nissen, E. Holdener, B. Speck, Treatment of thrombocytosis in myeloproliferative disorders with interferon alpha-2a. *Blut* **58**, 15–19 (1989).
12. M. O. Holmström, M. D. Hjortsø, S. M. Ahmad, Ö. Met, E. Martinenaite, C. Riley, P. Straten, I. M. Svane, H. C. Hasselbalch, M. H. Andersen, The *JAK2V617F* mutation is a target for specific T-cells in the *JAK2V617F* positive myeloproliferative neoplasms. *Leukemia* **31**, 495–498 (2017).
13. A. Mullally, S. W. Lane, B. Ball, C. Megerdichian, R. Okabe, F. Al-Shahrour, M. Paktinat, J. E. Haydu, E. Housman, A. M. Lord, G. Wernig, M. G. Kharas, T. Mercher, J. L. Kutok, D. G. Gilliland, B. L. Ebert, Physiological *Jak2V617F* expression causes a lethal myeloproliferative neoplasm with differential effects on hematopoietic stem and progenitor cells. *Cancer Cell* **17**, 584–596 (2010).
14. S. P. Gorantla, T. N. Dechow, R. Grundler, A. L. Illert, C. M. Zum Büschenfelde, M. Kremer, C. Peschel, J. Duyster, Oncogenic JAK2V617F requires an intact SH2-like domain for constitutive activation and induction of a myeloproliferative disease in mice. *Blood* **116**, 4600–4611 (2010).
15. T. M. Schnöder, P. Arreba-Tutusaus, I. Griehl, L. Bullinger, M. Buschbeck, S. W. Lane, K. Döhner, C. Plass, D. B. Lipka, F. H. Heidel, T. Fischer, Epo-induced erythroid maturation is dependent on Plcγ1 signaling. *Cell Death Differ.* **22**, 974–985 (2015).
16. S. E. Flanagan, E. Haapaniemi, M. A. Russell, R. Caswell, H. L. Allen, E. De Franco, T. J. McDonald, H. Rajala, A. Ramelius, J. Barton, K. Heiskanen, T. Heiskanen-Kosma, M. Kajosaari, N. P. Murphy, T. Milenkovic, M. Seppänen, Å. Lernmark, S. Mustjoki, T. Otonkoski, J. Kere,

N. G. Morgan, S. Ellard, A. T. Hattersley, Activating germline mutations in *STAT3* cause early-onset multi-organ autoimmune disease. *Nat. Genet.* **46**, 812–814 (2014).
17. M. Onishi, T. Nosaka, K. Misawa, A. L.-F. Mui, D. Gorman, M. McMahon, A. Miyajima, T. Kitamura, Identification and characterization of a constitutively active STAT5 mutant that promotes cell proliferation. *Mol. Cell. Biol.* **18**, 3871–3879 (1998).
18. A. Garcia-Diaz, D. S. Shin, B. H. Moreno, J. Saco, H. Escuin-Ordinas, G. A. Rodriguez, J. M. Zaretsky, L. Sun, W. Hugo, X. Wang, G. Parisi, C. P. Saus, D. Y. Torrejon, T. G. Graeber, B. Comin-Anduix, S. Hu-Lieskovan, R. Damoiseaux, R. S. Lo, A. Ribas, Interferon receptor signaling pathways regulating PD-L1 and PD-L2 expression. *Cell Rep.* **19**, 1189–1201 (2017).
19. W. J. C. Rombouts, I. Blokland, B. Löwenberg, R. E. Ploemacher, Biological characteristics and prognosis of adult acute myeloid leukemia with internal tandem duplications in the Flt3 gene. *Leukemia* **14**, 675–683 (2000).
20. C. Allen, R. K. Hills, K. Lamb, C. Evans, S. Tinsley, R. Sellar, M. O'Brien, J. L. Yin, A. K. Burnett, D. C. Linch, R. E. Gale, The importance of relative mutant level for evaluating impact on outcome of *KIT*, *FLT3* and *CBL* mutations in core-binding factor acute myeloid leukemia. *Leukemia* **27**, 1891–1901 (2013).
21. B. Gerstmayer, B. Groner, W. Wels, B. S. Schnierle, Stable expression of the ecotropic retrovirus receptor in amphotropic packaging cells facilitates the transfer of recombinant vectors and enhances the yield of retroviral particles. *J. Virol. Methods* **81**, 71–75 (1999).
22. F. Delhommeau, S. Dupont, C. Tonetti, A. Massé, I. Godin, J.-P. Le Couedic, N. Debili, P. Saulnier, N. Casadevall, W. Vainchenker, S. Giraudier, Evidence that the *JAK2* G1849T (V617F) mutation occurs in a lymphomyeloid progenitor in polycythemia vera and idiopathic myelofibrosis. *Blood* **109**, 71–77 (2007).
23. J. C. Wang, A. Kundra, M. Andrei, S. Baptiste, C. Chen, C. Wong, H. Sindhu, Myeloid-derived suppressor cells in patients with myeloproliferative neoplasm. *Leuk. Res.* **43**, 39–43 (2016).
24. F. Passamonti, F. Cervantes, A. M. Vannucchi, E. Morra, E. Rumi, A. Pereira, P. Guglielmelli, E. Pungolino, M. Caramella, M. Maffioli, C. Pascutto, M. Lazzarino, M. Cazzola, A. Tefferi, A dynamic prognostic model to predict survival in primary myelofibrosis: A study by the IWG-MRT (International Working Group for Myeloproliferative Neoplasms Research and Treatment). *Blood* **115**, 1703–1708 (2010).
25. S. Hasan, C. Lacout, C. Marty, M. Cuingnet, E. Solary, W. Vainchenker, J.-L. Villeval, $JAK2^{V617F}$ expression in mice amplifies early hematopoietic cells and gives them a competitive advantage that is hampered by IFNα. *Blood* **122**, 1464–1477 (2013).
26. C. Schultze-Florey, S. Raha, S. Ravens, L. Kuhlmann, M. Drenker, L. Oberdörfer, A. Breithaupt, E. Dammann, L. Hambach, M. Stadler, M. Heuser, F. Thol, R. Foerster, A. Ganser, I. Prinz, C. Koenecke, TCR diversity is a predictive marker for donor lymphocyte infusion response. *Blood* **128**, 4605 (2016).
27. B. Sido, J. Braunstein, R. Breitkreutz, C. Herfarth, S. C. Meuer, Thiol-mediated redox regulation of intestinal lamina propria T lymphocytes. *J. Exp. Med.* **192**, 907–912 (2000).
28. A. K. Sikalidis, Amino acids and immune response: A role for cysteine, glutamine, phenylalanine, tryptophan and arginine in T-cell function and cancer? *Pathol. Oncol. Res.* **21**, 9–17 (2015).
29. B. Sido, F. Lasitschka, T. Giese, N. Gassler, B. Funke, J. Schröder-Braunstein, U. Brunnemer, S. C. Meuer, F. Autschbach, A prominent role for mucosal cystine/cysteine metabolism in intestinal immunoregulation. *Gastroenterology* **134**, 179–191 (2008).
30. M. Nakaya, Y. Xiao, X. Zhou, J.-H. Chang, M. Chang, X. Cheng, M. Blonska, X. Lin, S.-C. Sun, Inflammatory T cell responses rely on amino acid transporter ASCT2 facilitation of glutamine uptake and mTORC1 kinase activation. *Immunity* **40**, 692–705 (2014).
31. M. D. Buck, D. O'Sullivan, E. L. Pearce, T cell metabolism drives immunity. *J. Exp. Med.* **212**, 1345–1360 (2015).
32. M. Marzec, Q. Zhang, A. Goradia, P. N. Raghunath, X. Liu, M. Paessler, H. Y. Wang, M. Wysocka, M. Cheng, B. A. Ruggeri, M. A. Wasik, Oncogenic kinase NPM/ALK induces through STAT3 expression of immunosuppressive protein CD274 (PD-L1, B7-H1). *Proc. Natl. Acad. Sci. U.S.A.* **105**, 20852–20857 (2008).
33. S. J. Wölfle, J. Strebovsky, H. Bartz, A. Sähr, C. Arnold, C. Kaiser, A. H. Dalpke, K. Heeg, PD-L1 expression on tolerogenic APCs is controlled by STAT-3. *Eur. J. Immunol.* **41**, 413–424 (2011).
34. M. L. Burr, C. E. Sparbier, Y.-C. Chan, J. C. Williamson, K. Woods, P. A. Beavis, E. Y. N. Lam, M. A. Henderson, C. C. Bell, S. Stolzenburg, O. Gilan, S. Bloor, T. Noori, D. W. Morgens, M. C. Bassik, P. J. Neeson, A. Behren, P. K. Darcy, S.-J. Dawson, I. Voskoboinik, J. A. Trapani, J. Cebon, P. J. Lehner, M. A. Dawson, CMTM6 maintains the expression of PD-L1 and regulates anti-tumour immunity. *Nature* **549**, 101–105 (2017).
35. R. Mezzadra, C. Sun, L. T. Jae, R. Gomez-Eerland, E. de Vries, W. Wu, M. E. W. Logtenberg, M. Slagter, E. A. Rozeman, I. Hofland, A. Broeks, H. M. Horlings, L. F. A. Wessels, C. U. Blank, Y. Xiao, A. J. R. Heck, J. Borst, T. R. Brummelkamp, T. N. M. Schumacher, Identification of CMTM6 and CMTM4 as PD-L1 protein regulators. *Nature* **549**, 106–110 (2017).
36. E. B. Garon, N. A. Rizvi, R. Hui, N. Leighl, A. S. Balmanoukian, J. P. Eder, A. Patnaik, C. Aggarwal, M. Gubens, L. Horn, E. Carcereny, M.-J. Ahn, E. Felip, J.-S. Lee, M. D. Hellmann, O. Hamid, J. W. Goldman, J.-C. Soria, M. Dolled-Filhart, R. Z. Rutledge, J. Zhang, J. K. Lunceford, R. Rangwala, G. M. Lubiniecki, C. Roach, K. Emancipator, L. Gandhi; KEYNOTE-001 Investigators, Pembrolizumab for the treatment of non-small-cell lung cancer. *N. Engl. J. Med.* **372**, 2018–2028 (2015).
37. J. E. Rosenberg, J. Hoffman-Censits, T. Powles, M. S. van der Heijden, A. V. Balar, A. Necchi, N. Dawson, P. H. O'Donnell, A. Balmanoukian, Y. Loriot, S. Srinivas, M. M. Retz, P. Grivas, R. W. Joseph, M. D. Galsky, M. T. Fleming, D. P. Petrylak, J. L. Perez-Gracia, H. A. Burris, D. Castellano, C. Canil, J. Bellmunt, D. Bajorin, D. Nickles, R. Bourgon, G. M. Frampton, N. Cui, S. Mariathasan, O. Abidoye, G. D. Fine, R. Dreicer, Atezolizumab in patients with locally advanced and metastatic urothelial carcinoma who have progressed following treatment with platinum-based chemotherapy: A single-arm, multicentre, phase 2 trial. *Lancet* **387**, 1909–1920 (2016).
38. H. Zhan, Y. Ma, C. H. S. Lin, K. Kaushansky, $JAK2^{V617F}$-mutant megakaryocytes contribute to hematopoietic stem/progenitor cell expansion in a model of murine myeloproliferation. *Leukemia* **12**, 2332–2341 (2016).
39. S. M. Koopmans, H. C. Schouten, A. M. W. van Marion, Anti-apoptotic pathways in bone marrow and megakaryocytes in myeloproliferative neoplasia. *Pathobiology* **81**, 60–68 (2014).
40. H. Yang, C. Bueso-Ramos, C. DiNardo, M. R. Estecio, M. Davanlou, Q.-R. Geng, Z. Fang, M. Nguyen, S. Pierce, Y. Wei, S. Parmar, J. Cortes, H. Kantarjian, G. Garcia-Manero, Expression of PD-L1, PD-L2, PD-1 and CTLA4 in myelodysplastic syndromes is enhanced by treatment with hypomethylating agents. *Leukemia* **28**, 1280–1288 (2014).
41. M. S. Davids, H. T. Kim, P. Bachireddy, C. Costello, R. Liguori, A. Savell, A. P. Lukez, D. Avigan, Y.-B. Chen, P. McSweeney, N. R. LeBoeuf, M. S. Rooney, M. Bowden, C. W. Zhou, S. R. Granter, J. L. Hornick, S. J. Rodig, M. Hirakawa, M. Severgnini, F. Stephen Hodi, C. J. Wu, V. T. Ho, C. Cutler, J. Koreth, D. Phil, E. P. Alyea, J. H. Antin, P. Armand, H. Streicher, E. D. Ball, J. Ritz, A. Bashey, R. J. Soiffer, Leukemia and Lymphoma Society Blood Cancer Research Partnership, Ipilimumab for patients with relapse after allogeneic transplantation. *N. Engl. J. Med.* **375**, 143–153 (2016).

Acknowledgments: *Pd-1*$^{-/-}$ mice on a C57BL/6 background were provided by R. Schrimbeck (Universitätsklinikum Ulm, Germany). The conditional floxed JAK2 (*JAK2FLEX/+* or *L2/+*) knock-in mice on C57Bl/6 background were a gift from J. L. Villeval (INSERM, U.1009, Villejuif, France). **Funding:** This study was supported by European Research Council Consolidator grant 681012 GvHDCure to R.Z., Deutsche Forschungsgemeinschaft (DFG) (Heisenberg Professorship ZE872/3-2 to R.Z., SFB1160/P14 to R.Z., P1 to S.E., SFB850/Z1 to H.B. and M.B., TRR167-NeuroMAC to R.Z., EXC-306 to H.B., MI1942/2-1 to S.M., and DKH 111764 to N.v.B.), Excellence Initiative (DFG, GSC-4, Spemann Graduate School of Biology and Medicine) scholarship to J.S.J., MSCA-ITN-2015-ETN-ALKATRAS (A.L.I.), NIH R01 CA72669 and P01 AI056299 to B.R.B., Bundesministerium für Bildung, Wissenschaft, Forschung und Technologie (Germany) (BMBF) to M.B. and S.E. (e:Med research), BMBF 01EO1303, DeCaRe (FKZ 01ZX1409B), DFG 2508/4-1 (N.v.B.), and Max Planck Society (E.L.P.). E.R. was supported by a fellowship by Associazione Italiana per la Ricerca sul Cancro cofunded by the European Union. **Author contributions:** A.P. and A.J.E. helped develop the overall concept, performed experiments, analyzed data, and helped write the manuscript; K.A. analyzed human BM samples; D.O. performed metabolism experiments and analyzed data; S.P.G. helped with the JAK2 BM transfection model; S.D. and W.M. helped with multiple experiments; L.B. performed Western blots; S.V. analyzed $JAK2^{V617F}$-mutant mice; M.B. and H.B. performed and analyzed array data; S.H. helped with transfection experiments; S.P. analyzed PB smears; T.P. performed transfection experiments; P.A. collected patient data; P.V. helped with luciferase promoter assay; M.H., M.B., and G.N. performed and analyzed PET/CT imaging; K.S. helped with luciferase promoter assays; J.S.J. helped with the Cre/lox-MPN model; J.W. collected clinical data; C.D. provided help/vital reagents; H.B. collected clinical data; A.S.-G. performed histology analysis; M.F. helped with fluorescence-activated cell sorting (FACS) experiments; D.P. analyzed microarray experiments and $JAK2^{V617F}$ allele burden; J.R., S.F., and S.E. provided help with STAT GOF/LOF; F.A.H. and S.M. helped with in vitro T cell analyses; C.M. helped with luciferase promoter assays; F.H.H. helped with EPO-R-tg 32D cells; N.K. and I.T. provided patient data; T.B. helped with cloning experiments; J.F. provided patient data; A.L.I. supervised oncogene-cloning experiments; J.D. and H.L.P. helped plan and analyze experiments; E.R. and C.B. performed and analyzed TCR sequencing; S.W.L. and G.R.H. provided JAK2-tg mice and supervised FACS experiments; B.R.B. provided vital reagents and analyzed data; E.L.P. planned and analyzed metabolism experiments; and R.Z. developed the overall study concept and planned experiments, analyzed data, and wrote the first draft of the manuscript. N.v.B. helped to plan experiments, provided reagents, and analyzed data. **Competing interests:** The authors declare that they have no competing interests. **Data and materials availability:** Microarray data are deposited in the database ArrayExpress (accession number E-MTAB-5028).

Submitted 14 January 2017
Resubmitted 19 September 2017
Accepted 8 December 2017
Published 21 February 2018
10.1126/scitranslmed.aam7729

Citation: A. Prestipino, A. J. Emhardt, K. Aumann, D. O'Sullivan, S. P. Gorantla, S. Duquesne, W. Melchinger, L. Braun, S. Vuckovic, M. Boerries, H. Busch, S. Halbach, S. Pennisi, T. Poggio, P. Apostolova, P. Veratti, M. Hettich, G. Niedermann, M. Bartholomä, K. Shoumariyeh, J. S. Jutzi, J. Wehrle, C. Dierks, H. Becker, A. Schmitt-Graeff, M. Follo, D. Pfeifer, J. Rohr, S. Fuchs, S. Ehl, F. A. Hartl, S. Minguet, C. Miething, F. H. Heidel, N. Kröger, I. Triviai, T. Brummer, J. Finke, A. L. Illert, E. Ruggiero, C. Bonini, J. Duyster, H. L. Pahl, S. W. Lane, G. R. Hill, B. R. Blazar, N. von Bubnoff, E. L. Pearce, R. Zeiser, Oncogenic $JAK2^{V617F}$ causes PD-L1 expression, mediating immune escape in myeloproliferative neoplasms. *Sci. Transl. Med.* **10**, eaam7729 (2018).

Science Translational Medicine

Oncogenic JAK2^{V617F} causes PD-L1 expression, mediating immune escape in myeloproliferative neoplasms

Alessandro Prestipino, Alica J. Emhardt, Konrad Aumann, David O'Sullivan, Sivahari P. Gorantla, Sandra Duquesne, Wolfgang Melchinger, Lukas Braun, Slavica Vuckovic, Melanie Boerries, Hauke Busch, Sebastian Halbach, Sandra Pennisi, Teresa Poggio, Petya Apostolova, Pia Veratti, Michael Hettich, Gabriele Niedermann, Mark Bartholomä, Khalid Shoumariyeh, Jonas S. Jutzi, Julius Wehrle, Christine Dierks, Heiko Becker, Annette Schmitt-Graeff, Marie Follo, Dietmar Pfeifer, Jan Rohr, Sebastian Fuchs, Stephan Ehl, Frederike A. Hartl, Susana Minguet, Cornelius Miething, Florian H. Heidel, Nicolaus Kröger, Ioanna Triviai, Tilman Brummer, Jürgen Finke, Anna L. Illert, Eliana Ruggiero, Chiara Bonini, Justus Duyster, Heike L. Pahl, Steven W. Lane, Geoffrey R. Hill, Bruce R. Blazar, Nikolas von Bubnoff, Erika L. Pearce and Robert Zeiser

Sci Transl Med **10**, eaam7729.
DOI: 10.1126/scitranslmed.aam7729

Cancers JAK up an immune checkpoint

Myeloproliferative neoplasms, a group of hematologic cancers, are associated with mutations activating the *JAK2* oncogene. *JAK2* is located on chromosome 9, in the vicinity of the immunosuppressive *PD-L1* gene, and Prestipino *et al.* discovered that myeloproliferative cancers with overactive JAK2 generally have increased PD-L1 as well. Although PD-L1 helps cancers evade the immune system, immune checkpoint inhibitors developed in recent years provide a way to block its function and turn PD-L1 expression into a therapeutic vulnerability for the tumors, as the authors demonstrate in this study.